12-1-2008

Consistency check of planned adaptive option on helical tomotherapy.

M Schirm

S Yartsev

G Bauman

Jerry J. Battista Dr.
University of Western Ontario, j2b@uwo.ca

Jacob Van Dyk
The University of Western Ontario, vandyk@uwo.ca

Technology in Cancer Research and Treatment
ISSN 1533-0346
Volume 7, Number 6, December 2008

Consistency Check of Planned Adaptive® Option on Helical Tomotherapy

www.tcrt.org

Maximilien Schirm[1]
Slav Yartsev, Ph.D.[1,2,*]
Glenn Bauman, MD[1,2]
Jerry Battista, Ph.D.[1,2]
Jake Van Dyk, M.Sc.[1,2]

[1]London Regional Cancer Program
London Health Sciences Center
790 Commissioners Road East
London, Ontario, Canada
[2]The University of Western Ontario
London, Ontario, Canada

This study aims to evaluate a new Planned Adaptive® software (TomoTherapy Inc., Madison, WI) of the helical tomotherapy system by retrospective verification and adaptive re-planning of radiation treatment. Four patients with different disease sites (brain, nasal cavity, lungs, prostate) were planned in duplicate using the diagnostic planning kVCT data set and MVCT studies of the first treatment fraction with the same optimization parameters for both plan types. The dosimetric characteristics of minimum, maximum, and mean dose to the targets as well as to organs at risk were compared. Both sets of plans were used for calculation of dose distributions in a water-equivalent phantom. Corresponding measurements of these plans in phantom were carried out with the use of radiographic film and ion chamber. In the case of the lung and prostate cancer patients, changes in dosimetric parameters compared to data generated with the kVCT study alone were less than 2%. Certain changes for the nasal cavity and brain cancer patients were greater than 2%, but they were explained in part by anatomy changes that occurred during the time between kVCT and MVCT studies. The Planned Adaptive software allows for adaptive radiotherapy planning using the MVCT studies obtained by the helical tomotherapy imaging system.

Key words: Helical tomotherapy; Adaptive radiotherapy; MVCT.

Introduction

Helical tomotherapy (HT) (TomoTherapy Inc, Madison, WI) is a form of image guided radiation therapy in which a linear accelerator is mounted on a slip ring gantry, similar to those used in helical CT scanners (1-6). During radiation treatment, the patient is translated through the gantry while the beam continually rotates around the patient, providing helical delivery. Using the same x-ray source, operated at 3.5 MV, megavoltage CT (MVCT) images can be acquired before, during, or after daily treatment of the patient (7, 8). The MVCT acquisition is currently used at our center for daily image registration with the planning kVCT (Brilliance Big Bore, Philips) dataset [see example in Fig. 1 (a)] and, thus, allows accurate patient re-positioning prior to daily treatments. These MVCT studies also provide new and exciting opportunities for adaptive radiotherapy (ART) (9, 10) by verification of delivered dose and replanning of patients throughout their coarse of treatment.

The new Planned Adaptive® software (TomoTherapy Inc, Madison, WI) provides tools for both dose verification and ART using the daily MVCT images acquired

[*]Corresponding Author:
Slav Yartsev, Ph.D.
Email: slav.yartsev@lhsc.on.ca

Abbreviations: ART, Adaptive radiation therapy; CT, Computed tomography; kVCT, Kilovoltage computed tomography; CTV, Clinical target volume; DVH, Dose volume histogram; MVCT, Megavoltage computed tomography; OAR, Organ at risk; PTV, Planned target volume; RED, Relative electron density.

by helical tomotherapy system. The MVCT study is always limited to a 40 cm circle of reconstruction due to the maximum tomotherapy collimator width whereas kVCT studies usually have a 50 cm circle of reconstruction (Brillaince Big Bore provides reliable CT numbers for up to 60 cm circle of reconstruction). Also MVCT scans are typically shorter in craniocaudal direction to save time and reduce the imaging dose. In order to compensate for insuffient field-of-view of the MVCT studies and accurately calculate dose, Planned Adaptive inserts the 40 cm round MVCT images into the kVCT planning study by creating a merged MVCT/kVCT image set, hencefore called "hybrid image", for convenience. Since kVCT studies are obtained with a slice thickness of 3 mm, and MVCT scanning on tomotherapy has possible slice spacing of 6, 4, or 2 mm, interpolation within the MVCT is required in order for the slice thickness of the merged image to be a uniform 3 mm thickness. A different image-value-density table (IVDT) is also required for dose calculations performed using MVCT images due to the higher beam energy of the tomotherapy unit.

Previous studies have shown that significant tumor regression may occur throughout treatment (9, 11-14) and in some cases, organs at risk (OARs) may move into high dose regions, thus delivering more dose than initially planned for critical tissue or underdosage of tumor volumes (11). By adapting the plan to these changes, the OARs can be spared of this inadvertent high dose deposition (15). Such adaptation also provides opportunities to increase organ sparing beyond what was initially planned, or to escalate dose delivered to the tumor while maintaining the same conformal avoidance of OARs if there is significant tumor regression during treatment. The question of using pre-treatment images for planning has been studied for another on-board imaging device, kV cone-beam CT, by Ding *et al*. (16, 17).

Clinically, Planned Adaptive provides unique opportunities for both dose verification and adaptive planning using the hybrid images already available. Dose verification allows for dosimetric assessment of the effects of misalignment or anatomy changes, while adaptive planning, when used in conjunction with the verification doses, allows for the adaptation of plans if the deformation or regression is considered clinically significant. However, the current software does not correct for the effects of anatomical deformation on dose delivered to individual tissue elements (18).

Previously an evaluation of the Planned Adaptive software has been done for phantom (19). The purpose of this study is to assess quantitatively the accuracy of this software using hybrid images for cases from our clinical practice. This was performed by retrospectively planning of four patients who had been treated on tomotherapy using both their initial kVCT and their *first* day MVCT studies, assuming no changes in patient anatomy occurred between these two studies. Multi-fraction dose accumulation was not studied in this preliminary work. The intent was to evaluate the possibility to employ hybrid images for dose delivery verification and adaptive therapy prior to their clinical usage.

Methods and Materials

Four patients with cancerous lesions at different sites (lung, prostate, nasal cavity, and brain) who had previously been treated at the London Regional Cancer Program using helical tomotherapy were selected retrospectively. A new hybrid image based plan was generated employing the same dosimetric constraints used for the original HT plan. This along with identical pitch, field width, modulation factor, and number of optimization iterations insures that the same planning procedure is implemented for both kVCT and hybrid image plans. The plans were optimized using the beamlet dose computation option.

Using the actual MVCT study of the first treatment day of each patient, hybrid images were created using the Planned Adaptive software. The number of scanned MVCT slices is defined by the minimum requirement of the PTV coverage. Radiation oncologist may require imaging of some easily identifiable anatomic feature or organ at risk. In practice, it means around 20 MVCT slices with 6 mm interslice spacing. Verification doses were calculated for each patient and compared to the planned doses. To accomplish this, Planned Adaptive applies the daily delivery sinogram (based on the original kVCT plan) in the calculation of the dose distribution on the current hybrid image. In clinical practice, it is intended that after dose verification calculations, summation doses (taking into account previously delivered fractions to tissue elements) are generated. Once a summation dose has been calculated, Planned Adaptive can allow for the modification of structures (including the generation of avoidance or "top up" regions based on patterns of accumulated dose that may have resulted in over- or under-dosage), and the hybrid image set with modified structures are transferred to the tomotherapy planning station for optimization of an "adaptive" plan to tailor the further treatments to correct for changes that have occurred up to that point in treatment. Depending on the clinical scenario, additional verifications and adaptive plans can be generated to correct for further anatomy changes (*i.e*., continued weight loss or tumor regression, internal anatomy warping). However, our current goal was not to test adaptive function as such but rather to see how close are the plan based on kVCT image with corresponding IVDT and the plan based on the hybrid image with IVDT for 3.5 MV beam.

In this study, we sought to verify that plan calculated on the hybrid image obtained with the *first* MVCT correlates well with the initial kVCT based plan. MVCT of the first day of

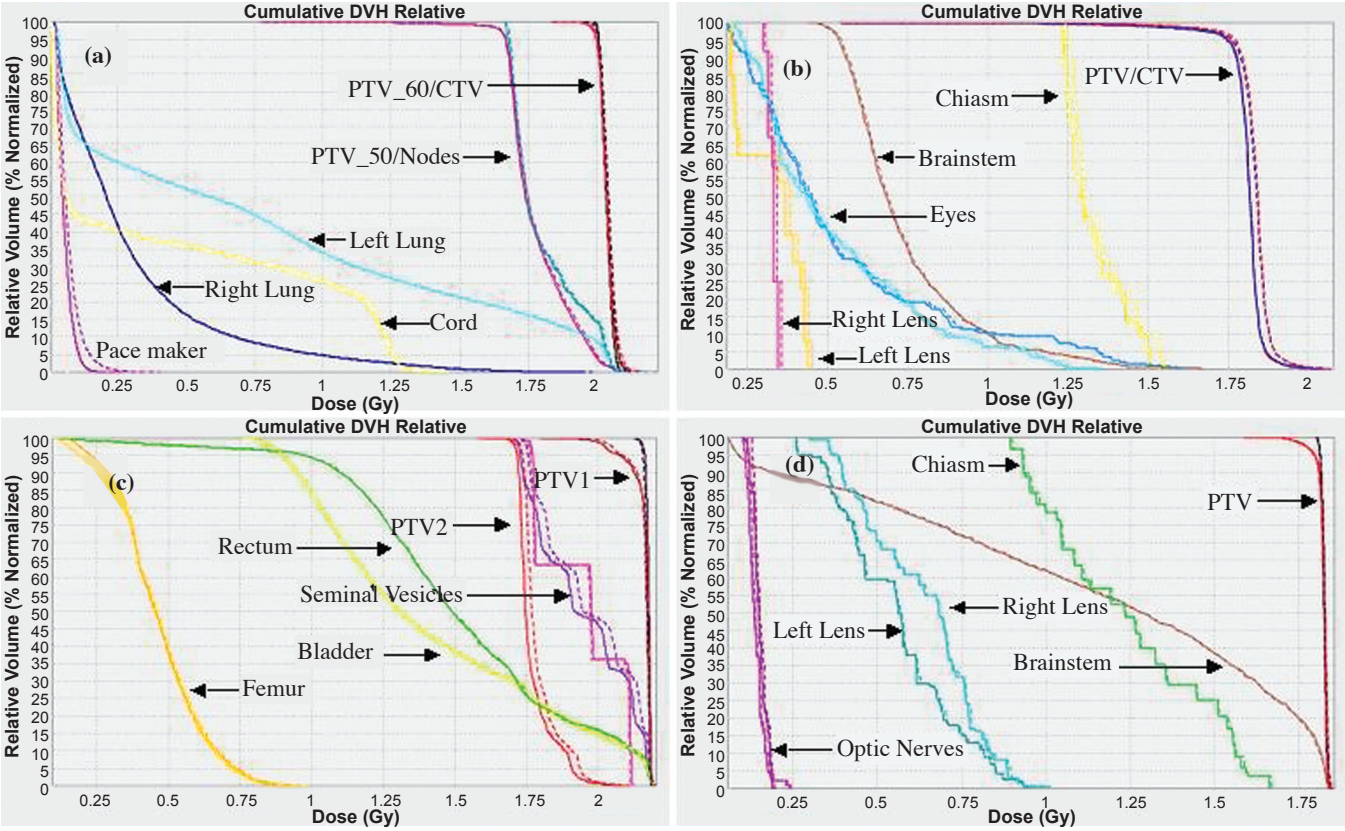

Figure 1: Verification dose volume histograms calculated on first day MVCT study for (**a**) lung cancer patient, (**b**) nasal cavity cancer patient, (**c**) prostate cancer patient, and (**d**) brain cancer patient. The solid lines are the DVH curves as planned, while the dashed lines are the verification DVH curves as calculated on the MVCT study. Superposition of the two sets of curves indicates equivalency of verification dose and planned dose.

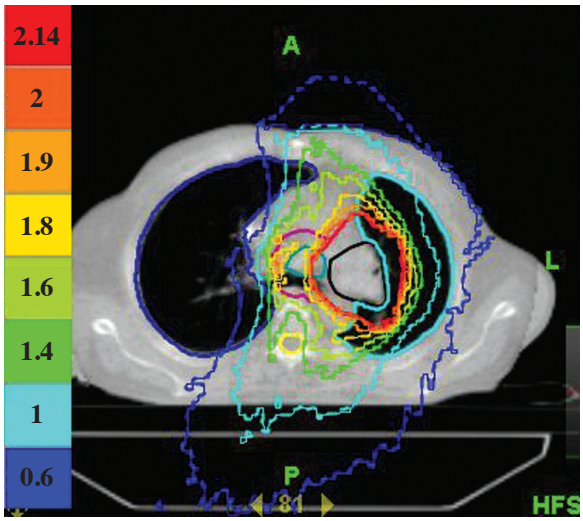

Figure 2: Hybrid image for the lung cancer patient with planned on kVCT study (solid lines) and calculated using hybrid image (dashed lines) isodose lines.

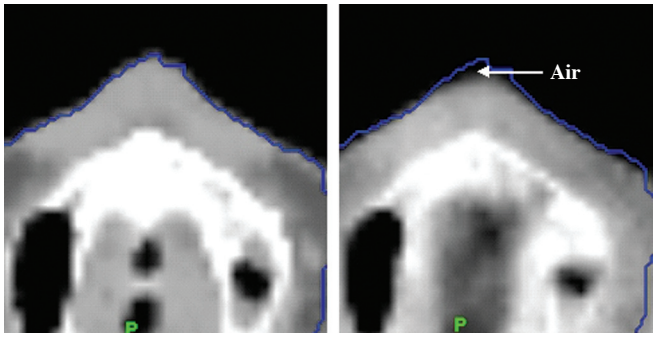

Figure 3: A slight deformation causes the minimum dose in PTV to be improperly calculated.

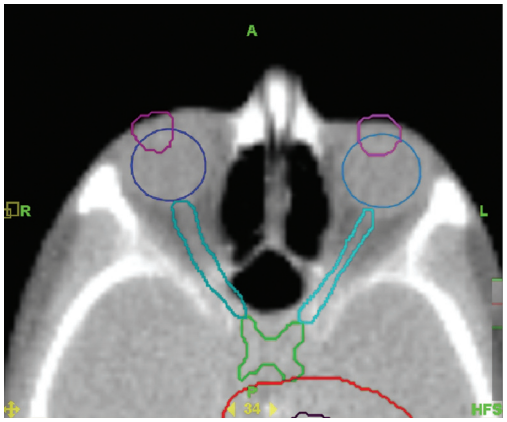

Figure 4: kVCT/MVCT hybrid image of brain cancer patient with a part of the lens contoured outside of patient.

treatment was chosen because we assumed that no significant changes in anatomy occurred after kVCT scan and the contours for all structures were kept the same for kVCT and hybrid image based plans. In doing so, one would have in-

Table I
Dosimetric parameters for lung cancer patient.

Structure	Plan	Max Dose[Gy]	Min Dose[Gy]	Median Dose[Gy]	Avg Dose[Gy]
PTV50	*kVCT plan*	61.44	43.34	51.78	51.90
	Hybrid image plan	61.67	43.82	51.83	51.95
	Percent difference	0.37	1.11	0.10	0.10
PTV60	*kVCT plan*	63.99	51.97	62.05	61.87
	Hybrid image plan	63.86	52.05	62.07	61.91
	Percent difference	0.20	0.15	0.03	0.06
RT Lung	*kVCT plan*	52.75	0.50	9.14	10.09
	Hybrid image plan	52.94	0.51	9.15	10.10
	Percent difference	0.36	2.00	0.11	0.10
LT Lung	*kVCT plan*	63.72	0.62	20.75	24.99
	Hybrid image plan	63.62	0.62	20.87	25.09
	Percent difference	0.16	0.00	0.58	0.40
Cord	*kVCT plan*	41.40	0.18	1.84	8.81
	Hybrid image plan	41.54	0.18	1.86	8.86
	Percent difference	0.34	0.00	1.09	0.57
Pace Maker	*kVCT plan*	2.73	1.01	1.47	1.53
	Hybrid image plan	2.74	1.02	1.48	1.54
	Percent difference	0.37	0.99	0.68	0.65

creased confidence that adaptive plans generated later after multi-fraction radiation delivery, based on the hybrid image alone would be truly reflective of subsequent adapted delivery. Isodose contours and dose volume histogram (DVH) curves were used to quantify the differences between the plans. Each hybrid image plan was directly compared to the kVCT plan in order to determine the effects of the inherent lower quality of MVCT images due to the higher beam energy.

To verify the calculation accuracy, delivery quality assurance (DQA) procedures were performed for all patients as an independent verification of the plans. Radiographic film and ion chamber point dose measurements with a cylindrical water equivalent "cheese" phantom were performed for both kVCT and hybrid image based plans. In order to correct for any differences due to set-up or organ motion error (and in doing so isolate the effects of differences in the planning as opposed to the anatomy), the hybrid image for adaptive planning was corrected by the automated registration shifts used for the first day of treatment.

Results

Figure 1 shows the comparison of DVHs as planned (solid

Table II
Dosimetric parameters for prostate patient.

Structure	Plan	Max Dose[Gy]	Min Dose[Gy]	Median Dose[Gy]	Avg Dose[Gy]
PTV2	*kVCT plan*	77.30	63.47	76.71	76.26
	Hybrid image plan	77.20	63.48	76.68	76.22
	Percent difference	0.13	0.02	0.04	0.05
PTV1	*kVCT plan*	74.32	56.00	61.58	62.44
	Hybrid image plan	74.25	55.99	61.58	62.40
	Percent difference	0.09	0.02	0.00	0.06
Seminal Vesicles	*kVCT plan*	77.16	60.20	67.70	68.81
	Hybrid image plan	77.12	60.07	67.66	68.77
	Percent difference	0.05	0.22	0.06	0.06
Bladder	*kVCT plan*	77.11	26.24	45.87	49.80
	Hybrid image plan	77.10	26.26	45.78	49.77
	Percent difference	0.01	0.08	0.20	0.06
Rectum	*kVCT plan*	77.16	4.27	47.38	49.78
	Hybrid image plan	77.13	4.23	47.57	49.97
	Percent difference	0.04	0.94	0.40	0.38
Penile Bulb	*kVCT plan*	74.85	60.79	69.75	68.85
	Hybrid image plan	74.73	61.25	69.82	68.92
	Percent difference	0.16	0.76	0.10	0.10

Table III
Dosimetric parameters for nasal cavity patient.

Structure	Plan	Max Dose[Gy]	Min Dose[Gy]	Median Dose[Gy]	Avg Dose[Gy]
PTV	*kVCT plan*	40.13	11.31	35.99	35.81
	Hybrid image plan	40.21	10.34	36.03	35.85
	Percent difference	0.20	8.58	0.11	0.11
Left Lens	*kVCT plan*	8.39	3.79	7.21	6.25
	Hybrid image plan	8.34	3.73	7.07	6.18
	Percent difference	0.60	1.58	1.94	1.12
Lt Eye	*kVCT plan*	31.93	3.60	8.18	10.19
	Hybrid image plan	32.28	3.53	8.19	10.15
	Percent difference	1.10	1.94	0.12	0.39
Rt Eye	*kVCT plan*	26.00	4.08	7.67	9.72
	Hybrid image plan	26.22	4.07	7.89	9.78
	Percent difference	0.85	0.25	2.87	0.62
Brainstem	*kVCT plan*	32.43	7.89	12.55	13.70
	Hybrid image plan	32.30	7.80	12.51	13.60
	Percent difference	0.40	1.14	0.32	0.73
Chiasm	*kVCT plan*	29.12	23.18	24.83	25.40
	Hybrid image plan	29.28	23.15	24.88	25.29
	Percent difference	0.55	0.13	0.20	0.43

lines) with those calculated with the "verification dose" option of the Planned Adaptive software for each of the patients by applying the kVCT generated fluence map to the first day hybrid image.

The results of kVCT vs. hybrid image based plans are presented in Tables I to IV where the maximum, minimum, median, and average dose for six selected structures were compared for the lung, prostate, nasal cavity, and brain cancer patients. A maximum of 2% difference between the plan using the merged image and the plan using the kVCT planning image for each parameter of the structures used for comparison was considered clinically acceptable. Figure 2 shows a lung cancer patient isodose view illustrated on the hybrid image with kVCT study visible outside 40 cm MVCT circle. We observe good agreement between planned (on kVCT study) and calculated (using hybrid) image isodose lines for a delivery fraction. DQA procedures of tomotherapy system were also used for both kVCT and hybrid image plans. Point dose measurements provided quantitative comparison shown in Table V. Film isodose contours exhibited good agreement for all plans, and most point dose measurements agreed within 2% with those predicted by the corresponding plan. In certain cases, point dose measurement differences

Table IV
Dosimetric parameters for brain cancer patient.

Structure	Plan	Max Dose[Gy]	Min Dose[Gy]	Median Dose[Gy]	Avg Dose[Gy]
PTV	*kVCT plan*	54.74	50.22	54.41	54.36
	Hybrid image plan	54.77	50.22	54.38	54.34
	Percent difference	0.05	0.00	0.06	0.04
Lt Optic Nerve	*kVCT plan*	33.28	11.47	23.27	22.00
	Hybrid image plan	33.20	10.91	23.29	21.75
	Percent difference	0.24	4.88	0.09	1.14
RT Optic Nerve	*kVCT plan*	31.75	12.12	19.14	19.86
	Hybrid image plan	31.95	12.07	19.24	19.99
	Percent difference	0.63	0.41	0.52	0.65
Lt Lens	*kVCT plan*	9.17	4.14	5.57	5.73
	Hybrid image plan	8.81	3.77	5.02	5.20
	Percent difference	3.93	8.94	9.87	9.25
Rt Lens	*kVCT plan*	10.12	4.96	7.81	7.87
	Hybrid image plan	9.87	4.47	7.58	7.57
	Percent difference	2.47	9.88	2.94	3.81
Chiasm	*kVCT plan*	51.51	30.83	43.46	42.08
	Hybrid image plan	51.63	31.26	43.14	42.03
	Percent difference	0.23	1.39	0.74	0.12

Table V
Delivery quality assurance point dose measurements.

Patient	Structure	kVCT Calc Dose [Gy]	Hybrid image Calc Dose [Gy]	Difference (%)	kVCT Meas Dose [Gy]	Hybrid image Meas Dose [Gy]	Difference (%)
Lung	Tumor	1.782	1.786	0.2	1.742	1.748	0.3
	Rt Lung	0.475	0.479	0.8	0.441	0.447	1.4
	Cord	1.041	1.046	0.5	1.026	1.014	-1.2
Nasal Cavity	Tumor	0.883	0.894	1.2	0.905	0.905	0.0
	Rt. Eye	0.296	0.290	-2.0	0.277	0.296	6.9
Brain	Tumor	1.376	1.374	-0.1	1.416	1.421	0.4
	Tumor	1.374	1.377	0.2	1.416	1.415	-0.1
	Rt. Eye	0.268	0.264	-1.5	0.304	0.313	3.0
Prostate	Tumor	2.884	2.852	-1.1	2.826	2.803	-0.8
	Bladder	1.389	1.378	-0.8	1.318	1.340	1.7
	Rectum	1.227	1.182	-3.7	1.226	1.203	-1.9

exceeded 2% due to either the low delivered dose or the high dose gradient in this region.

Discussion

The verification dose of the nasal cavity patient (see Fig. 1b), when compared to the planned dose, shows small differences most notably for the optic chiasm, the planning target volume (PTV) and clinical target volume (CTV). The fine structures, such as nasal cavities, on the MVCT images are blurred due to the lower image quality of the hybrid image study. The blurring results in changes of CT numbers in corresponding voxels, which may affect the dose calculation. This effect likely accounts for the difference (clinically insignificant) in the optic chiasm DVH concordance. In our case, MVCT images were acquired with coarse (6 mm) slice spacing. In the future, we plan to study the effect of scanning with smaller interslice distances on the image quality and how this improves verification dose calculations. In this instance, interfaces between bone and air represent a high contrast situation, thus improvements through adjustment of slice thickness may improve the correspondence between plans. In addition, small discrepancies in the registration that resulted in portions of the PTV residing in air (Fig. 3) help account for the discrepancy as they result in a calculated underdosage of this portion of the PTV given the lack of soft tissue buildup. This suggests that in using adaptive planning for targets that are on the surface, careful review of the planning contours to ensure there is appropriate mapping to the current surface is necessary.

The hybrid image based plan for the prostate cancer patient showed agreement to better than 1% for all parameters when compared to the kVCT plan (Fig. 1c). Due to the nature of the region, this is to be expected: while the region is not of uniform density, only the femurs and portions of the rectum show large differences in atomic number and densities. The majority of the contoured structures in the case of prostate cancer patients are large enough such that image noise, artifacts, and blurring are averaged and do not affect the plan in any significant manner. With structures of similar density arranged in proximity, it is possible that the delineation of the structures on MVCT images may be more difficult (20). Despite this concern, we noted high concordance between the PTV1 (prostate only) DVH between the kVCT and hybrid image plans suggesting contouring differences between the two studies was not an issue. Likewise, good concordance between the rectal and bladder DVHs suggested minimal organ deformation between the kVCT and hybrid images. There was a noticeable difference between the verification dose and the planned dose for the PTV2 and seminal vesicle structures as shown in Figure 1c. The seminal vesicles are more mobile than the prostate and may be more subject to subtle changes in bladder and rectum volume leading to variation of dose deposition in the small (and hence more sensitive to tissue modification) volumes such as the seminal vesicle and PTV2 contours. To account for this deformation, modification of the structures should be performed, although in this preliminary study we assumed that no modification to the structures occurs between time of kVCT and hybrid images on the first day of treatment. Alternatively, repeating the comparison with kVCT and hybrid image done in closer temporal proximity (*i.e.*, sequentially) may reduce this discrepancy by reducing the possibility of changes in rectal and bladder filling between studies (21).

There was concern that breathing motion induced artifacts may lead to some errors in dose calculations in the case of the lung cancer patients (22); however, our data for this particular case did not show this. In this case the tumor is attached to mediastunum and probably does not move much. The results in Figure 1a and Table I may indicate that the motion induced artifacts, which could be different in the fast (gantry rotation speed of 0.5 s in kVCT) and slow (gantry rotation speed of 10 s in MVCT), or the blurring of motion, had not changed the dose distributions significantly. If proved for a

larger cohort of lung cancer patients (or alternatively if the upper limit for tumor motion is defined), such insensitivity to motion artifacts could be very useful for adaptive radiotherapy. In some cases of lung cancer, the tumor will regress throughout treatment (12-14), allowing for further sparing of the ipsilateral lung, the contralateral lung, the heart, the spinal cord, and other OARs. With less dose delivered to the OARs, complications, such as radiation pneumonitis and esophagitis, are less likely to occur, thus increasing the overall quality of life of the patients.

The minimum dose to the PTV for the nasal cavity cancer patient in Table III showed almost a 9% difference, while the remaining characteristics were below the 2% threshold. The discrepancy is due to a portion of PTV in air (Fig. 3).

In the case of the brain cancer patient, there were significant differences in the dose calculations for lenses and the left optic nerve, while the PTV, right optic nerve, and optic chiasm all showed excellent agreement. Once again, with structures close to the surface a significant portion of both lenses are contoured outside of the patient and in air on the merged image, causing the dose calculations for these structures located near the surface of the patient to be significantly different (Fig. 4). In the case of the left optic nerve, the minimum dose may be affected by the blurring of the fine structures when using MVCT images with 6 mm slice spacing and interpolation. Quantifying the differences in the delineation of fine structures for head and neck cases in 6, 4, and 2 mm slice spacing would allow for the best choice in slice spacing to be made for adaptive planning purposes. It may be that a policy of 6 mm scanning for daily localization with a repeat finer (2 or 4 mm scan) scan for adaptive planning (if concerning anatomy trends are noted on the routine localization scanning) would be a good compromise between daily treatment efficiency and dose accuracy for adaptive re-planning.

Conclusions

In the case of the lung and prostate cancer patients, there is good agreement in the calculations of the verification doses and excellent agreement in the comparison of the hybrid image based plans to the kVCT plans. In these cases, the contoured structures are well within the patient; therefore there are no adverse effects due to surface dose calculations or patient deformation. The structures in both these cases are also fairly large, allowing for image noise and poor contrast to be averaged out. In both the nasal cavity and brain cancer patients, structures near the surface of the patient caused some discrepancies in dose calculations on the hybrid image plan due to small differences between the images. Due to the decrease in quality of the MVCT image, fine anatomic structures are not as visible, and may cause some discrepancies in dose calculations. Use of finer resolution MVCT scans for adaptive planning in these scenarios may be advisable.
Clinically, verification doses can be used to assess the dose delivered to patient over the course of treatment and are useful in determining if anatomical changes are clinically relevant. This can be accomplished by adapting structures on the hybrid image to account for anatomy changes. Since these patient images are already available, calculation of verification doses offer an additional quality assurance option for patients treated on tomotherapy. If the anatomical changes are clinically relevant, Planned Adaptive supplies tools with which adaptive plans can be created. Future work will focus on verifying multi-fraction adaptive plans. By using Planned Adaptive in conjunction with the planning station, more conformal radiation therapy may be possible, along with dose escalation, further sparing of critical structures, and consequently, higher uncomplicated survival rates.

Acknowledgements

We are thankful to Drs. A. R. Dar, B. Fisher, and G. Rodrigues for providing patient data. This study was conducted with the support of the Ontario Institute for Cancer Research through funding provided by the government of Ontario.

References

1. Fenwick, J. D., Tome, W. A., Kissick, M. W., Mackie, T. R. Modelling simple helically delivered dose distributions. *Phys Med Biol 50*, 1505-1517 (2005).
2. Jeraj, R., Mackie, T. R., Balog, J., Olivera, G., Pearson, D., Kapatoes, J., Ruchala, K., Reckwerdt, P. Radiation characteristics of helical tomotherapy. *Med Phys 31*, 396-404 (2004).
3. Mackie, T. R., Balog, J., Ruchala, K., Shepard, D., Aldridge, S., Fitchard, E., Reckwerdt, P., Olivera, G., McNutt, T., Mehta, M. Tomotherapy. *Sem Radiat Oncol 9*, 108-117 (1999).
4. Mackie, T. R. History of tomotherapy. *Phys Med Biol 51*, R427-R453 (2006).
5. Tomsej, M. Le système de tomothérapie hélicoïdale pour la radiothérapie modulée en intensité et guidée par l'image: développements récents et applications cliniques. *Cancer/Radiothér 10*, 288-295 (2006).
6. Welsh, J. S., Patel, R. R., Ritter, M. A., Harari, P. M., Mackie, T. R., Mehta, M. P. Helical tomotherapy: an innovative technology and approach to radiation therapy. *Technol Canc Res Treat 1*, 311-316 (2002).
7. Meeks, S. L., Harmon Jr., J. F., Langen, K. M., Willoughby, T. R., Wagner, T. H., Kupelian, P. A. Performance characterization of megavoltage computed tomography imaging on a helical tomotherapy unit. *Med Phys 32*, 2673-2681 (2005).
8. Ruchala, K. J., Olivera, G. H., Schloesser, E. A., Mackie T, R, 1999 Megavoltage CT on a tomotherapy system. *Phys Med Biol 44*, 2597-2621 (1999).
9. Ramsey, C. R., Langen, K. M., Kupelian, P. A., Scaperoth, D. D., Meeks, S. L., Mahan, S. L., Seibert, R. M. A technique for adaptive image-guided helical tomotherapy for lung cancer. *Int J Radiat Oncol Biol Phys 64*. 1237-1244 (2006).
10. Welsh, J. S., Lock, M., Harary, P., Tomé, W. Clinical implementation of adaptive helical tomotherapy: A unique approach to image-guided intensity modulated radiotherapy. *Technol Canc Res Treat 5*, 465-480 (2006).

11. Roach, M., Faillace-Akazawa, P., Malfatti, C. Prostate volumes and organ movement defined by serial computerized tomographic scans during three-dimensional conformal radiotherapy. *Radiat Oncol Investigations 5*, 187-194 (1997).
12. Siker, M. L., Tomé, W. A., Mehta, M. P. Tumor volume changes on serial imaging with megavoltage CT for non-small-cell lung cancer during intensity-modulated radiotherapy: How reliable, consistent, and meaningful is the effect? *Int J Radiat Oncol Biol Phys 66*, 135-141 (2005).
13. Kupelian, P. A., Ramsey, C. R., Meeks, S. L., Willoughby, T. R., Forbes, A., Wagner, T. H., Langen, K. M. Serial megavoltage CT imaging during external beam radiotherapy for non-small-cell lung cancer: Observations on tumor regression during treatment. *Int J Radiat Oncol Biol Phys 63*, 1024-1028 (2005).
14. Yartsev, S., Dar, A. R., Woodford, C., Wong, E., Bauman, G., Van Dyk, J. Initial experience in treating lung cancer with helical tomotherapy. *Biomed Imaging Interv J 3*, e2 (2007).
15. Kuo, Y. C., Wu, T. H., Chung, T. S., Huang, K. W., Chao, K. S., Su, W. C., Chiou, J. F. Effect of regression of enlarged neck lymph nodes on radiation doses received by parotid glands during intensity-modulated radiotherapy for head and neck cancer. *Amer J Clin Oncol 29*, 600-605 (2006).
16. Ding, G. X., Duggan, D. M., Coffey, C. W., Deeley, M., Hallan, D. E., Cmelak, A., Malcolm, A. A study on adaptive IMRT treatment planning using cone-beam CT. *Radiother Oncol 85*, 116-125 (2007).
17. Ding, G. X., Duggan, D. M., Coffey, C. W. Accurate patient dosimetry of kilovoltage cone-beam CT in radiation therapy. *Med Phys 35*, 1135-1144 (2008).
18. Schaly, B., Kempe, J. A., Bauman, G. S., Battista, J. J., Van Dyk, J.Tracking the dose distribution in radiation therapy by accounting for variable anatomy. *Phys Med Biol 49*, 791-805 (2004).
19. Langen, K. M., Meeks, S. L., Poole, D. O., Wagner, T. H., Willoughby, T. R., Kupelian, P. A., Ruchala, K. J., Haimerl, J., Olivera, G. H. The use of megavoltage CT (MVCT) images for dose recomputations. *Phys Med Biol 50*, 4259-4276 (2005).
20. Song, W. Y., Chiu, B , Bauman, G. S., Lock, M., Rodrigues, G., Ash, R., Lewis, C., Fenster, A., Battista, J. J., Van Dyk, J. Prostate contouring uncertainty in megavoltage computed tomography images acquired with a helical tomotherapy unit during image-guided radiation therapy. *Int J Radiat Oncol Biol Phys 65*, 595-607 (2006).
21. Song,W., Schaly, B., Bauman, G., Battista, J.,Van Dyk, J. 2005 Image-guided adaptive radiation therapy (IGART): Radiobiological and dose escalation considerations for localized carcinoma of the prostate. *Med Phys 32*, 2193-2203 (2005).
22. Smeenk, C., Gaede, S., Battista, J. J. Delineation of moving targets with slow MVCT scans: implications for adaptive non-gated lung tomotherapy. *Phys Med Biol 52*, 1119-1134 (2007).

Received: May 23, 2008; Revised: September 30, 2008; Accepted: October 20, 2008